Eddy currents and corner singularities

François Buret, Monique Dauge, Patrick Dular, Laurent Krähenbühl, Victor Péron, Ronan Perrussel, Clair Poignard, Damien Voyer

Eddy currents and corner singularities

F. Buret*, M. Dauge¶, P. Dular†, L. Krähenbühl*, V. Péron‡, R. Perrussel‖, C. Poignard§, and D. Voyer*
*Laboratoire Ampère CNRS UMR5005, Université de Lyon, École Centrale de Lyon, Écully, France
¶IRMAR CNRS UMR6625, Université de Rennes 1, Rennes, France
†F.R.S.-FNRS, ACE research-unit, Université de Liège, Liège, Belgium
‡LMAP CNRS UMR5142, INRIA Bordeaux-Sud-Ouest, Team MAGIQUE-3D, Pau, France
‖LAPLACE CNRS UMR5213, Université de Toulouse, INPT-ENSEEIHT, Toulouse, France
§INRIA Bordeaux-Sud-Ouest, Team MC2, IMB CNRS UMR5251, Université Bordeaux 1, Talence, France

***Abstract*—Eddy current problems are addressed in this paper, in a bidimensional setting where the conducting medium is non-magnetic and has a corner singularity. For any fixed skin depth we show that the flux density $|\nabla A_\delta|$ is bounded near the corner, unlike the perfect conducting case. Then as the skin depth goes to zero, the first two terms of a multiscale expansion of the magnetic potential are introduced to tackle the magneto-harmonic problem. The heuristics of the method are given and numerical computations illustrate the obtained accuracy.**

***Index Terms*—eddy current problem, singularity, asymptotic expansion.**

I. Introduction

ELECTROTHERMIC applications require a precise knowledge of the Joule power density. Skin effect combined with corner singularities is an obstacle to reach this precision. Here, we introduce a method to tackle a magneto-harmonic problem in 2D where the conducting medium is *non-magnetic* and has a *corner singularity*. More precisely, denote by Ω_- the bounded domain corresponding to the conducting medium, and by Ω_+ the surrounding dielectric medium (see Fig. 1(a)). The domain Ω with boundary Γ is defined by $\Omega = \Omega_- \cup \Omega_+ \cup \Sigma$, where Σ is the boundary of Ω_-. For the sake of simplicity, we assume that:

(H1) Σ has only one geometric singularity, and we denote by C this corner. The angle of the corner (from the conducting material, see Fig. 1(a)) is denoted by ω.

(H2) the current source term J is located in Ω_+ and it vanishes in a neighborhood of C.

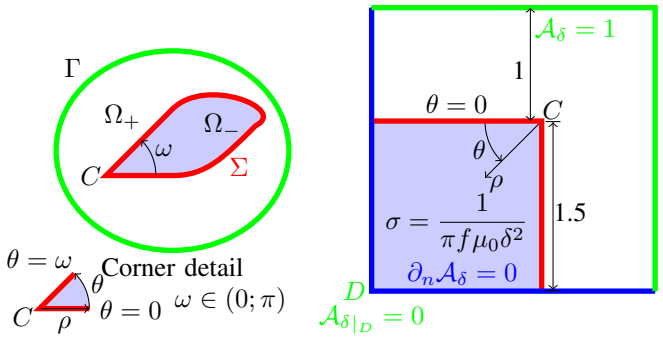

(a) Model domain for the heuristics. (b) L-shape dielectric domain and boundary conditions for the computations.

Fig. 1. Geometry of the considered problems.

Throughout the paper ρ denotes the distance to the corner C and θ is the angular variable (see Fig. 1). Moreover the notations $[u]_\Sigma = u^+|_\Sigma - u^-|_\Sigma$ and $\partial_n = n \cdot \nabla$ are used, n being the normal to Σ inwardly directed from Ω_+ to Ω_-. Denote by $\delta = \sqrt{1/(\pi f \sigma \mu_0)}$ the skin depth, where f is the frequency of the source term, σ is the conductivity, and μ_0 is the vacuum magnetic permeability. The magnetic vector potential $\mathcal{A}_\delta$ (reduced to a single scalar component in 2D) satisfies[1]

$$\begin{cases} -\Delta \mathcal{A}_\delta^+ = \mu_0 J \text{ in } \Omega_+, & \\ -\Delta \mathcal{A}_\delta^- + \dfrac{2\mathrm{i}}{\delta^2}\mathcal{A}_\delta^- = 0 \text{ in } \Omega_-, & [\mathcal{A}_\delta]_\Sigma = 0, \text{ on } \Sigma, \\ \mathcal{A}_\delta^+ = 0 \text{ on } \Gamma, & [\partial_n \mathcal{A}_\delta]_\Sigma = 0, \text{ on } \Sigma. \end{cases} \tag{1}$$

Two main insights are addressed in this paper: we first show in section II that for any given $\delta > 0$ the flux density $|\nabla \mathcal{A}_\delta|$ near the corner is *not singular* in the sense that it remains bounded. Elements are given in section II to understand the behavior of the solution, and numerical simulations illustrate the reasoning. Based on this fact, we then provide a method to approach $\mathcal{A}_\delta$ when δ is small compared with the characteristic length of the domain. Actually, for regular interface Σ the potential $\mathcal{A}_0$ solution to

$$\begin{cases} -\Delta \mathcal{A}_0^+ = \mu_0 J & \text{in } \Omega_+, \\ \mathcal{A}_0^+ = 0 & \text{on } \Sigma, \\ \mathcal{A}_0^+ = 0 & \text{on } \Gamma, \end{cases} \qquad \mathcal{A}_0^- = 0 \text{ in } \Omega_-, \tag{2}$$

intuitively approximates $\mathcal{A}_\delta$ in the dielectric medium and it can be proved that the "power norm" [1] of the error $\mathcal{A}_\delta - \mathcal{A}_0$ is of order δ [2]. However this accuracy is no more valid near a corner singularity since $\nabla \mathcal{A}_\delta$ is bounded whereas $\nabla \mathcal{A}_0$ blows up at the corner. Section III proposes the heuristics of a rigorous method to obtain the order δ by adding an appropriate correction in the neighborhood of the corner, and we conclude by numerical experiments.

Manuscript received July 7, 2011. Corresponding author: C. Poignard (e-mail: clair.poignard@inria.fr).
Digital Object Identifier inserted by IEEE.

[1]For simplicity, the generic framework of the analysis deals with homogeneous Dirichlet boundary condition in the dielectric, and a source term localized far from the corner. However mixed boundary conditions as described by Fig. 1(b), while they hold far from the corner, lead to similar results. For numerical simulations we deal with the configuration given by Fig. 1(b).

Note that Yuferev *et al.* in [3] have considered a similar problem using a formal approach of transmitted singularities. Their work aimed at "correcting" the method proposed by Deeley [4]. However we are confident that the heuristics of [3] lead to non-relevant results, since we show in section II-B that the impedance does not blow up near the corner as stated by equations (24)–(25) of [3].

II. Expansion of the solution close to the corner

In this section we suppose that δ is a *given* strictly positive parameter (we consider it as fixed) and we aim at giving a corner asymptotics of $\mathcal{A}_\delta$ as $\rho \to 0$. The corner asymptotics is the notion which generalizes the Taylor expansion to solutions to corner problems. By convention, the terms of such asymptotics are called *singularities*, even if it happens that they are polynomial functions. To simplify the notations, throughout this section ζ denotes $2\mathrm{i}/\delta^2$.

A. First singular functions of the eddy current problem

To determine the singular functions of the eddy current problem, we introduce the infinite sectors of same openings as in problem (1): (S_+, S_-) are the two sectors of $\mathbb{R}^2$ separated by $\mathcal{G}$ as

$$\begin{aligned} S_- &= \big\{X = (\rho\cos\theta, \rho\sin\theta)) \,:\, \rho > 0,\, |\theta| \le \omega/2\big\},\\ \mathcal{G} &= \partial S_- = \Big\{X \,:\, |\theta| = \frac{\omega}{2}\Big\},\\ S_+ &= \mathbb{R}^2 \setminus (S_- \cup \mathcal{G})\,. \end{aligned} \tag{3}$$

Near the corner, the operator of the eddy current problem is

$$\mathscr{L}(v) = \begin{cases} -\Delta v, \quad \text{in } S_+ \\ -\Delta v + \zeta v, \quad \text{in } S_- \\ [v]_{\mathcal{G}} = 0, \quad [\partial_\theta v]_{\mathcal{G}} = 0. \end{cases} \tag{4}$$

Thus $\mathscr{L}$ is the sum of its leading part $\mathscr{L}_0$ which is the Laplacian $-\Delta$ in $\mathbb{R}^2$, and of its secondary part $\zeta\mathscr{L}_1$ where $\mathscr{L}_1$ is the operator of restriction to S_-. According to the general principles of Kondratev's seminal paper [5], the singularities of $\mathscr{L} = \mathscr{L}_0 + \zeta\mathscr{L}_1$ are obtained by solving by induction the series of equations

$$\mathscr{L}_0\mathfrak{u}_0 = 0,\ \mathscr{L}_0\mathfrak{u}_1 = -\mathscr{L}_1\mathfrak{u}_0, \ldots, \mathscr{L}_0\mathfrak{u}_j = -\mathscr{L}_1\mathfrak{u}_{j-1}, \tag{5}$$

in spaces of quasi-homogeneous functions, i.e. functions of the form $\sum_q \rho^\lambda \log^q(\rho)\varphi_q(\theta)$. The number λ can be real or complex in general and is called singularity exponent. The singularities of $\mathscr{L}$ are then given by $\mathfrak{s} = \sum_j \zeta^j \mathfrak{u}_j$. The leading part of $\mathfrak{s}$ is $\mathfrak{u}_0$, solution to $\Delta\mathfrak{u}_0 = 0$ in $\mathbb{R}^2$. Since we are interested in singularity functions with finite energy (*i.e* the gradient is L^2), we restrict to positive exponents λ. Then $\mathfrak{u}_0$ are homogeneous *harmonic polynomials* in Cartesian variables and the numbers λ are the natural integers. We enumerate them as $(\mathfrak{u}_0^{k,p})_{k\in\mathbb{N},\,p=0,1}$ defined in polar coordinates by

$$\mathfrak{u}_0^{k,p}(\rho,\theta) = \rho^k \cos(k\theta - p\pi/2).$$

Note that $\mathfrak{u}_0^{k,1}(\rho,\theta) = \rho^k\sin(k\theta)$ and that it degenerates to 0 if $k = 0$. Each $\mathfrak{u}_0^{k,p}$ is the leading part of the singular function $\mathfrak{s}^{k,p}$. For $j \ge 1$ the next terms $\mathfrak{u}_j^{k,p}$ in the series (5) are the *shadow terms* and the function $\mathfrak{u}_j^{k,p}$ is a particular solution to the following problem in $\mathbb{R}^2$:

$$\begin{cases} \Delta\mathfrak{u}_j^{k,p\,+} = 0, \text{ in } S_+, \\ \Delta\mathfrak{u}_j^{k,p\,-} = \mathfrak{u}_{j-1}^{k,p}, \text{ in } S_-, \\ \left[\mathfrak{u}_j^{k,p}\right]_{\mathcal{G}} = 0,\ \left[\partial_\theta\mathfrak{u}_j^{k,p}\right]_{\mathcal{G}} = 0, \end{cases} \tag{6}$$

and then the singular function $\mathfrak{s}^{k,p}$ equals

$$\mathfrak{s}^{k,p}(\rho,\theta) = \sum_{j\ge 0} \zeta^j \mathfrak{u}_j^{k,p}(\rho,\theta) \quad \forall k \in \mathbb{N},\, p = 0, 1.$$

Complete description of the singular functions $\mathfrak{s}^{k,p}$ cannot be stated in this 4-page paper, however we provide here the first shadow term $\mathfrak{u}_1^{0,0}$ generated by $\mathfrak{u}_0^{0,0} = 1$. Solving (6) we find

$$\begin{aligned} \mathfrak{u}_1^{0,0}(\rho,\theta) = {}& \frac{\sin\omega}{4\pi}\rho^2\big(\log(\rho)\cos(2\theta) - \theta\sin(2\theta)\big) \\ & + \frac{\sin\omega}{4}\operatorname{sgn}(\theta)\rho^2\sin(2\theta) + \frac{\cos\omega}{4}\rho^2\cos(2\theta), \\ & \qquad \text{for } \theta \in [-\pi,\pi]\setminus[-\omega/2,\omega/2] \\ \mathfrak{u}_1^{0,0}(\rho,\theta) = {}& \frac{\sin\omega}{4\pi}\rho^2\big(\log(\rho)\cos(2\theta) - \theta\sin(2\theta)\big) + \frac{1}{4}\rho^2, \\ & \qquad \text{for } \theta \in (-\omega/2,\omega/2). \end{aligned}$$

Note that for each ρ, the function $\theta \mapsto \mathfrak{u}_1^{0,0}(\rho,\theta)$ is regular (infinitely differentiable) on $[-\pi,\pi]\setminus[-\omega/2,\omega/2]$ viewed as an interval of the torus.

Remark 2.1: One can prove that for any $k \in \mathbb{N}, p = 0, 1$, the j^{th}-order shadow function $\mathfrak{u}_j^{k,p}$ of $\mathfrak{u}_0^{k,p}$ behaves like $\rho^{k+2j}\log^j(\rho)$ as ρ goes to zero. This justifies that neither $\mathcal{A}_\delta$ nor $\nabla\mathcal{A}_\delta$ does blow up as ρ goes to zero, which is in contradiction with the assumption at equation (10) of [3].

B. Expansion of $\mathcal{A}_\delta$ and impedance near the corner

According to Kondratev's results [5], there exists complex numbers $(\Lambda^{k,p})_{k\in\mathbb{N},\,p=0,1}$ such that near the corner $\mathcal{A}_\delta$ can be expanded as

$$\mathcal{A}_\delta \sim_{\rho\to 0} \sum_{k\in\mathbb{N},\,p=0,1} \Lambda^{k,p}\mathfrak{s}^{k,p}(\rho,\theta). \tag{7}$$

The coefficient $\Lambda^{0,0}$ is nothing but the pointwise value $\mathcal{A}_\delta(C)$ of $\mathcal{A}_\delta$ at the corner C. All the coefficients $\Lambda^{k,p}$ depend on δ.

Let us use expansion (7) to find the form of the impedance function Z_δ on the interface. The function Z_δ is defined as

$$\frac{1}{2\mathrm{i}\pi f\mu_0} Z_\delta(\rho,\pm\omega/2) = \frac{\mathcal{A}_\delta(\rho,\pm\omega/2)}{\partial_n\mathcal{A}_\delta(\rho,\pm\omega/2)} = \frac{\rho\,\mathcal{A}_\delta(\rho,\pm\omega/2)}{\partial_\theta\mathcal{A}_\delta(\rho,\pm\omega/2)}.$$

We find the first-order expansion of Z_δ as $\rho \to 0$ using the first terms in (7):

$$\mathcal{A}_\delta = \mathcal{A}_\delta(C)\left(1 + \zeta\mathfrak{u}_1^{0,0}\right) + \sum_{k=1}^{2}\sum_{p=0}^{1}\Lambda^{k,p}\mathfrak{u}_0^{k,p} + o(\rho^2). \tag{8}$$

In particular, we emphasize that near the corner

$$\begin{aligned} \partial_n\mathcal{A}_\delta(\rho,\omega/2) = {}& -\Lambda^{1,0}\sin(\omega/2) + \Lambda^{1,1}\cos(\omega/2) \\ & - \zeta\rho\log(\rho)\mathcal{A}_\delta(C)\sin^2\omega/(2\pi) + O(\rho), \end{aligned}$$

and therefore near the corner the impedance becomes

$$Z_\delta(\rho,\omega/2) = \frac{2\mathrm{i}\pi f\mu_0\,\mathcal{A}_\delta(C)}{-\Lambda^{1,0}\sin(\omega/2)+\Lambda^{1,1}\cos(\omega/2)} + \frac{2\mathrm{i}\pi f\mu_0\,\zeta\rho\log(\rho)\left(\mathcal{A}_\delta(C)\sin\omega\right)^2}{2\pi\left(-\Lambda^{1,0}\sin(\omega/2)+\Lambda^{1,1}\cos(\omega/2)\right)^2} + O(\rho). \tag{9}$$

Therefore we have shown that as ρ goes to zero, the impedance tends to a constant and thus it does not blow up as $1/\rho$ as described in [3].

C. Numerical experiments

Observe the importance of the first shadow $\mathfrak{u}_1^{0,0}$ in (8), since its leading term is in $\rho^2\log(\rho)$, which is greater than ρ^2 as ρ goes to zero. We now present the computations that illustrate formula (8).

Solution to problem (1) is computed by finite element method in the configuration given by Fig. 1(b), with the skin depth equal to $\delta = 5\mathrm{mm}$, the length of the big square equal to $100\mathrm{mm}$ and the length of the small square equal to $50\mathrm{mm}$. Fig. 2 shows the isovalue line of $\Re(\mathcal{A}_\delta)$.

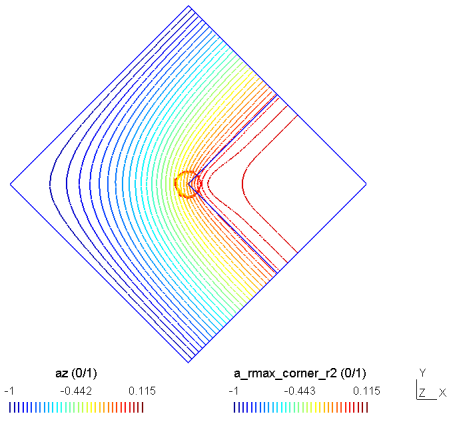

Fig. 2. Isovalue lines of the amplitude of the real part of the potential $\mathcal{A}_\delta$ computed by finite element method. The circle refers to the zone of Fig. 3

Near the corner, the finite element solution is compared with the numerical value[2] of $\mathcal{A}_\delta$ given by (8). In Fig. 3(a) and Fig. 3(b), an approximation of $\Re(\mathcal{A}_\delta)$ obtained with the help of (8) have been superposed to the numerical value of $\Re(\mathcal{A}_\delta)$ given by the finite element method. Fig 3(a) compares $\Re(\mathcal{A}_\delta)$ with the expression (8) without the terms $\Lambda^{2,p}\mathfrak{u}_0^{2,p}$, while Fig 3(b) compares $\Re(\mathcal{A}_\delta)$ with the full formula (8).

Observe in Fig. 3(a) that the isovalue lines of the approximation do not match accurately with the finite element solution, especially in the dielectric part of the neighborhood of the corner. This is due to the omitting of the terms $\Lambda^{2,p}\mathfrak{u}_0^{2,p}$, since as shown in Fig. 3(b) the matching is much better using all the terms of (8). Hence Fig. 3 illustrates the theoretical results given by (8).

[2]For $k = 1, 2$ and $p = 0, 1$, the coefficients $\Lambda^{k,p}$ of (8) are appoached for ρ_0 small enough, by

$$\Lambda^{k,p} \sim \frac{\rho_0^{-k}}{2\pi}\int_{-\pi}^{\pi}\left(\mathcal{A}_\delta(\rho_0,\theta) - \Lambda^{0,0}\zeta\mathfrak{u}_1^{0,0}(\rho_0,\theta)\right)\cos(k\theta - p\pi/2)\,\mathrm{d}\theta.$$

This formula will be explained in a forthcoming long paper but we chose to present it here so that the reader can verify the computations of Fig. 3.

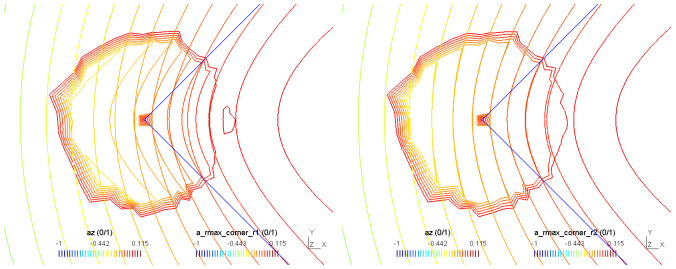

(a) The terms $\mathfrak{u}_0^{2,p}$ are omitted in (8). (b) Complete expression (8).

Fig. 3. Numerical comparison of the near corner real parts of $\mathcal{A}_\delta$ computed by finite element method and of its approximations given by (8).

III. Heuristics of the multiscale expansion

The next two sections deal with the behavior of $\mathcal{A}_\delta$, for δ tending to zero. Let first note the two following remarks:

- similarly to the regular case, $\mathcal{A}_0$ defined by (2) is the solution to the limit problem of (1) as δ goes to zero, at least far from the corner.

Hence the first term of the expansion should start by $\mathcal{A}_0$.

- since the respective behaviors of $\mathcal{A}_\delta$ and $\mathcal{A}_0$ are different at the corner for any non-zero δ, it is natural to truncate $\mathcal{A}_0$ by a radial function φ which is zero close to the corner and 1 far from it.

For $d_0 < d_1$ let φ and φ_δ be the cut-off functions:

$$\varphi(\rho) = \begin{cases} 1, & \text{if } \rho \geqslant d_1 \\ 0, & \text{if } \rho \leqslant d_0 \end{cases}, \quad \varphi(\cdot/\delta) : \rho \mapsto \varphi(\rho/\delta) \tag{10}$$

d_0, d_1 being fixed corner distances. As δ goes to zero the energy norm of the error $\mathcal{A}_\delta - \varphi\mathcal{A}_0$ does not go to zero in the disk of radius d_0, since φ vanishes and $\mathcal{A}_\delta$ does not. We intuite that $\varphi(\cdot/\delta)\mathcal{A}_0$ is the good approximation and the following results show this. Let $r_0^\delta = \mathcal{A}_\delta - \varphi(\cdot/\delta)\mathcal{A}_0$, it satisfies

$$-\Delta r_0^\delta = [\Delta;\varphi(./\delta)]\,\mathcal{A}_0^+, \text{ in } \Omega_+, \quad r_0^\delta|_\Gamma = 0, \text{ on } \Gamma, \tag{11a}$$

$$-\Delta r_0^\delta + \frac{2\mathrm{i}}{\delta^2} r_0^\delta = 0, \quad \text{in } \Omega_-, \tag{11b}$$

$$\left[r_0^\delta\right]_\Sigma = 0,\ \left[\partial_n r_0^\delta\right]_\Sigma = -\partial_n\left(\varphi(./\delta)\mathcal{A}_0^+\right), \quad \text{on } \Sigma, \tag{11c}$$

where for any couple (ν, u), $[\Delta;\nu]u = \Delta(\nu u) - \nu\Delta u$. Note assumption (H2) (see section I) is necessary to obtain (11a).

If we were not to use the cut-off function φ near the corner, therefore the jump $\left[\partial_n r_0^\delta\right]_\Sigma$ would be equal to $-\partial_n\mathcal{A}_0^+|_\Sigma$, which blows up at the corner. Since $[\partial_n\mathcal{A}_\delta]_\Sigma$ identically vanishes in the corner on Σ we would have to compensate this blowing term, which would lead to numerical difficulties. The use of $\varphi(./\delta)$ in (11c) ensures that $\left[\partial_n r_0^\delta\right]_\Sigma$ vanishes near the corner. Solving exactly (11) provides no benefits compared with the computation of (1), but we will take advantage of the knowledge of $\mathcal{A}_0^+$ near the corner:

$$\mathcal{A}_0^+ \underset{\rho\to 0}{\simeq} a_1\rho^\alpha\sin(\alpha(\theta-\omega/2)), \quad \text{where } \alpha = \frac{\pi}{2\pi-\omega}. \tag{12}$$

Insert (12) into such (11) and perform the rescaling $X = x/\delta$ ($R = \rho/\delta$). Let δ go to zero (Γ is thus "sent" to the infinite) to make appear the "profile" term V_α that is *independent of*

$\mathcal{A}_0$ *and* δ and satisfies in $\mathbb{R}^2$

$$-\Delta_X V_\alpha = [\Delta_X;\varphi]\left(R^\alpha \sin(\alpha(\theta-\omega/2))\right), \text{ in } S_+, \quad (13a)$$

$$-\Delta_X V_\alpha + 2\mathrm{i}V_\alpha = 0, \text{ in } S_-, \quad (13b)$$

$$[V_\alpha]_{\mathcal{G}} = 0, \quad [\partial_\theta V_\alpha]_{\mathcal{G}} = \alpha\varphi R^{\alpha-1}, \quad (13c)$$

$$V_\alpha \to_{|X|\to+\infty} 0, \quad (13d)$$

where S_+, S_- and $\mathcal{G}$ are defined by (3). Observe that near the corner, $a_1\delta^\alpha V_\alpha(./\delta)$ does not correct exactly (11c), however according to (12), it corrects its leading term, the other terms being neglected. Hence $\mathcal{A}_\delta$ writes

$$\mathcal{A}_\delta = \varphi\left(\frac{\cdot}{\delta}\right)\mathcal{A}_0 + (1-\varphi)a_1\delta^\alpha V_\alpha\left(\frac{\cdot}{\delta}\right) + r_\alpha^\delta. \quad (14)$$

The theoretical proof of the existence and uniqueness of V_α as well as the justification that r_α^δ is of order δ need more than 4 pages, and will be presented in a forthcoming long paper. Capturing the singularity of the domain in a profile term is quite natural and has to be linked up similarly to [6], [7].

IV. Numerical results

The domain presented in Fig. 1(b) is considered for the numerical purpose. The errors $|r_0^\delta|$ and $|r_\alpha^\delta|$ are plotted respectively in Fig. 4(a) and 4(b). The terms $\mathcal{A}_\delta$, a_1, $\mathcal{A}_0$ and V_α are computed by using the finite element method.The scalar potential $\mathcal{A}_\delta$ has been computed in the whole domain using a sufficiently fine mesh near the corner, to ensure the good accuracy of $\mathcal{A}_\delta$ and of its first order derivatives.

On both figures, the same color scale is used except the white area around the corner in Fig. 4(a) where the error is higher (between 0.04 and 0.14). Fig. 4(b) shows the profile correction (13): the highest error lies now in the regular part of the interface Σ, for which correction is known [2].

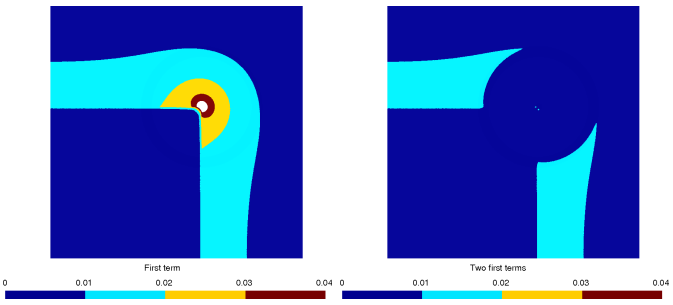

(a) $|r_0^\delta|$. (b) $|r_\alpha^\delta|$.

Fig. 4. Modulus of the errors between the solution and the two first orders of (14) for $\delta = 0.025$. The distances of (10) are $d_0 = 1$ and $d_1 = 1.2$.

Suppose that $a_1 \neq 0$, which is the worst corner influence, and denote by $Z_s = (1+\mathrm{i})/(\sigma\delta)$ the regular surface impedance. According to the expansion, the surface impedance Z_δ can be approximated close to the corner by:

$$Z_\delta = Z_s\frac{1+\mathrm{i}}{\delta}\frac{\mathcal{A}_\delta}{\partial_n\mathcal{A}_\delta} \underset{\rho\to 0}{\simeq} Z_s(1+\mathrm{i})\frac{V_\alpha(\cdot/\delta)}{(\partial_n V_\alpha)(\cdot/\delta)}, \quad (15)$$

therefore for any σ and f such that δ is small enough, the function $Z_\delta(\delta\cdot)/|Z_s|$ behaves close to zero as $\sqrt{2}\mathrm{i}V_\alpha/(\partial_n V_\alpha)$. These similar behaviors are shown in Fig. 5 where the "impedance" from the profile function is compared to the real impedance for two values of δ, where f and σ are different. According to [3], the surface impedance should blow up like ρ^{-1} for any non-zero δ, which is shown to be false here.

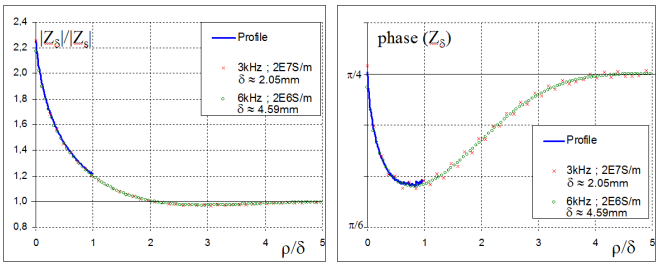

Fig. 5. Behavior of $Z_\delta/|Z_s|$ vs ρ/δ. The domain characteristic length L is here 0.1m, then δ/L is between 2 and 4.6% for the situations considered.

V. Conclusion

In conclusion, this paper aimed at providing efficient method to compute the eddy current problem in a domain with corner singularity. We have provided theoretical argument that shows that the flux density $|\nabla\mathcal{A}_\delta|$ does not blow up near the corner for any fixed $\delta > 0$, while $\nabla\mathcal{A}_0$ does, which is in accordance with the numerics. In particular equality (9) provides an approximation of the impedance condition near the corner. The main insights of the present paper are twofold. Firstly, (9) shows that for any non-zero skin depth, the impedance near the corner tends to a constant as ρ goes to zero instead of blowing up as $1/\rho$ as stated in [3]. Secondly, as δ goes to zero, we have introduced a profile term V_δ that captures the singularity of the domain in order to approach accurately $\mathcal{A}_\delta$ near the corner. Equality (15) shows that near the corner the impedance is no more intrinsic, unlike the case of regular interface, since the profile V_α depends on the angle opening.

For all these reasons, we emphasize that the use of impedance boundary conditions should be drastically prohibited in domains with geometric singularity, and multi-scale expansion as described in section III should be preferred.

References

[1] K. Schmidt, O. Sterz, and R. Hiptmair, "Estimating the Eddy-Current modeling error," *IEEE Trans. on Mag.*, vol. 44, no. 6, pp. 686–689, 2008.

[2] G. Caloz, M. Dauge, and V. Péron, "Uniform estimates for transmission problems with high contrast in heat conduction and electromagnetism," *Journal of Mathematical Analysis and Applications*, vol. 370, no. 2, pp. 555–572, 2010.

[3] S. Yuferev, L. Proekt, and N. Ida, "Surface impedance boundary conditions near corner and edges: Rigorous consideration," *IEEE Trans. on Mag.*, vol. 37, no. 5, pp. 3465–3468, 2001.

[4] E. Deeley, "Surface impedance near edges and corners in three-dimensional media," *IEEE Trans. on Mag.*, vol. 26, no. 2, pp. 712–714, 1990.

[5] V. A. Kondrat′ev, "Boundary value problems for elliptic equations in domains with conical or angular points," *Trudy Moskov. Mat. Obšč.*, vol. 16, pp. 209–292, 1967.

[6] I. Ciuperca, R. Perrussel, and C. Poignard, "Influence of a Rough Thin Layer on the Steady-state Potential," *IEEE Trans. on Mag.*, vol. 46, no. 8, pp. 2823–2826, 2010.

[7] L. Krähenbühl, F. Buret, R. Perrussel, D. Voyer, P. Dular, V. Péron, and C. Poignard, "Numerical treatment of rounded and sharp corners in the modeling of 2D electrostatic fields," *Journal of microwaves, optoelectronics and electromagnetic applications*, vol. 10, no. 1, pp. 66–81, 2011.